Angle-resolved photoemission theory for valence electrons. I. A calculation scheme by the multi-slice method

1993 J. Phys.: Condens. Matter 5 8211

(http://iopscience.iop.org/0953-8984/5/44/012)

J. Phys.: Condens. Matter 5 (1993) 8211–8224. Printed in the UK

Angle-resolved photoemission theory for valence electrons: I. A calculation scheme by the multi-slice method

C Stampfl†, K Kambe†, J D Riley‡ and D F Lynch§

† Fritz-Haber-Institut der Max-Planck-Gesellschaft, Faradayweg 4-6, D-14 195 Berlin (Dahlem), Federal Republic of Germany

‡ Department of Physics, La Trobe University, Bundoora 3083, Australia

§ CSIRO Division of Materials Science and Technology, Clayton 3168, Australia

Received 18 June 1993, in final form 16 August 1993

Abstract. A one-step photoemission calculation scheme for valence electrons is presented which uses (to construct the initial- and final-state wavefunctions) the multi-slice technique, which has been developed for low-energy electron diffraction (LEED). Included in the scheme is the possibility of having an over-layer or an arbitrarily shaped surface barrier, and realizing both the electron and hole life-times by means of an imaginary part to the energy. The photoemission intensity due to surface states can also be calculated separately by the same procedure. The advantage of the scheme is that because the crystal potential is divided into arbitrarily thin slices, problems associated with the frequently used muffin-tin potential do not arise.

1. Introduction

To interpret experimental photoemission data it is necessary to have an underlying theory. The three-step model developed by Berglund and Spicer [1] has proved to be a very useful method which has been compared successfully with experimental data [2]. However, certain features are observed in experimental data that cannot be described by this model, for example, emission from surface states and resonances, and accurate intensities of bulk transitions. The three-step model is limited to direct transitions and because of the exact conservation of the electron wave vector, it does not deal with the width of direct transition lines [3].

A more quantitative way to treat the photoemission process, which takes full account of the one-electron bandstructure, multiple scattering of the photoelectron, lifetime broadening and surface effects, is the one-step model of photoemission, where an electron is excited out of its initial state directly into its final state. Various one-step theories have been given in the literature [4–26]; the more recent ones being based on Pendry's [26, 27] non-relativistic layer-KKR photoemission theory, which can also be used to calculate inverse photoemission intensities [28]. The one-step theory has been steadily improved and extended over the years by several groups. In particular, a realistic model for the surface potential has been introduced [15–19] as have relativistic [20–22] and temperature effects [23, 24]. Recently, this scheme has been generalized to the case of space-filling potential cells of arbitrary shape [25] which means that the muffin-tin approximation need not be used. While the muffin-tin approximation is particularly suited to close-packed systems, more open and covalent structures are not well described.

In this paper we present an alternative approach using pseudopotentials. The calculation uses LEED techniques to construct explicitly the initial and final states which are written as a

0953-8984/93/448211+14$07.50

linear combination of Bloch waves. The LEED scheme combines the semi-reciprocal method of Tournarie [29] with the multi-slice method of Cowley and Moodie [30]. By considering a very thin slice of crystal, the solution can be given analytically. The full solution can then be obtained as the product of solutions for individual slices (the Ω-matrix method).

In most photoemission calculations the crystal is divided into layers containing an arrangement of coplanar atoms, whose potential is chosen to be a muffin-tin potential. The slicing of the potential, as is done in the calculation scheme presented here, means that no such restriction is incurred, so that it is possible to calculate the photoemission for complicated structures, including surface barriers and over-layers. The drawback of the present method is that because a pseudopotential must be used for the calculation of the initial states to keep the amount of numerical work feasible, photoemission intensities from core levels cannot be obtained directly. Also, one should keep in mind that the obtained initial-state wavefunctions are not the true ones, but pseudowavefunctions. It was shown by Martinez *et al* [31] that the values of the squares of the matrix elements are approximately 10–20% too small in comparison with the values obtained by using more accurate wavefunctions. In our calculations, however, we are not aiming at obtaining the intensities with a better accuracy than this. The level of agreement with experimental results can be seen in section 3. The inaccuracies introduced by using pseudowavefunctions may depend on the material and the pseudopotential used.

In the present paper the theoretical method is given, with one numerical example of calculated photoemission intensities for Mg(0001) in section 3. Further results obtained using the method outlined here are presented in the succeeding papers [32, 33]. In a previous paper [34], it has been shown that complex bulk and surface state/resonance bandstructures can be obtained with a satisfactory accuracy using the multi-slice method, where bandstructures were obtained for Mg and GaAs.

2. Method

This section presents the derivation of the equations used to calculate the photoemission intensities. The photocurrent in a one-step model can be written, within the one-electron picture, as

$$j(\hat{R}, E) \propto \sum_{\text{occupied } i} |\langle \psi_f(r, \hat{R}, E) | H^{\text{int}} | \psi_i(r) \rangle|^2 \delta(E - E_i - \hbar\omega) \qquad (1)$$

where E_i is the energy of the initial state and ψ_i is the occupied eigenstate. $\hat{R}$ is the position vector of the detector and ψ_f and E are the final state and energy of the photoelectron respectively. The interaction of the electrons with the exciting electromagnetic field is taken as [35]

$$H^{\text{int}} = -(i\hbar e/2mc) A_0 \hat{\varepsilon} \cdot \nabla$$

where $\hat{\varepsilon}$ is the polarization vector and A_0 is the magnitude of the vector potential of the incident light field.

It is easier to understand the photoemission calculation if the method of solution of LEED intensities is understood. This is described in detail in [34] and [36] and outlined below in section 2.1.

2.1. LEED calculation

The Schrödinger equation for LEED can be written as

$$\nabla^2\psi^{\mathrm{L}} + (2m/\hbar^2)(E - V)\psi^{\mathrm{L}} = 0. \tag{2}$$

The superscript L denotes LEED. The crystal potential is represented by a Fourier summation, where the coefficients $V(h, k, l)$ are the structure factors

$$V(x, y, z) = \sum_{h,k,l} V(h, k, l) \exp(\mathrm{i}\boldsymbol{r} \cdot \boldsymbol{g}_{h,k,l}) \tag{3}$$

and

$$V(h, k, l) = \sum_{j=1}^{n} f_j(g_{h,k,l}) \exp(\mathrm{i}\boldsymbol{d}_j \cdot \boldsymbol{g}_{h,k,l}). \tag{4}$$

f_j is the atomic form factor and $\boldsymbol{d}_j$ is the position vector of the ion j in the unit cell. $\boldsymbol{g}_{h,k,l}$ is a reciprocal lattice vector, h, k, l being indices, and $\boldsymbol{r}$ is the real space vector. Equation (2) can be expressed in mixed representation, that is, reciprocal space is used in the plane parallel to the surface (the x, y plane) by imposing Bloch periodicity for given values of $(k_x, k_y) = \boldsymbol{k}_{\|}$, but not in the direction z perpendicular to the surface. The LEED wavefunction in real space can then be written as

$$\psi^{\mathrm{L}}(x, y, z) = \exp(\mathrm{i}\boldsymbol{k}_{\|}^{\mathrm{L}} \cdot \boldsymbol{\rho}_{\|}) \sum_{h,k} \Psi_{h,k}^{\mathrm{L}}(z) \exp[2\pi\mathrm{i}(h\boldsymbol{b}_1 + k\boldsymbol{b}_2) \cdot \boldsymbol{\rho}_{\|}] \tag{5}$$

where $\boldsymbol{k}_{\|}^{\mathrm{L}}$ is determined from the angle and energy of the LEED electron, $\boldsymbol{\rho}_{\|} = (x, y)$, and $\boldsymbol{b}_{1,2}$ are the surface reciprocal lattice vectors. We call $\Psi_{h,k}^{\mathrm{L}}$ the scattering amplitudes. The Schrödinger equation can then be expressed as a first order matrix equation by using a supermatrix and solved for $\Psi_{h,k}^{\mathrm{L}}$ by using the Ω-matrix method [34].

The number of $\Psi_{h,k}^{\mathrm{L}}(z)$ is truncated to a suitable value N. This value may be taken as the number of reciprocal lattice rods intersecting the Ewald sphere inside the crystal, or a larger number of rods may be taken where the extra rods correspond to evanescent waves in the crystal. Equivalently, N can be thought of as the number of 'beams'; $2N$ being the number of plane waves in the two-dimensional expansion of the wavefunction.

The scattering amplitude $\Psi_{h,k}^{\mathrm{L}}(z)$ in the bulk region is written as a linear combination of Bloch wave amplitudes. A LEED solution for a sufficiently thick slab is known *a priori* to include only the Bloch functions decreasing into the bulk. For a particular h, k

$$\Psi_{h,k}^{\mathrm{L}}(z) = \sum_{n} {}^{\mathrm{L}}b_{h,k}^{n}(z) t_n^{\mathrm{L}} \tag{6}$$

where ${}^{\mathrm{L}}b_{h,k}^{n}(z)$ are the amplitudes associated with the beam (h, k) derived from the nth Bloch wave travelling into the crystal (that is, decreasing with increasing z), and the t_n^{L} are the coefficients to be determined from the boundary conditions incorporating the surface region properly [34].

2.2. Final states

The final states of the photoemission process are determined directly from the LEED calculation. The final states are the time-reversed states of the LEED states described in section 2.1. The final state can be written as a Fourier expansion as shown in equation (5) for the LEED wavefunction, but with superscript f, denoting the photoelectron final state, instead of L. The scattering amplitude $\Psi^{\mathrm{f}}_{h,k}(z)$ can be expressed as a linear combination of Bloch waves as in the LEED case shown in equation (6), but again with superscript f. The LEED state ψ^{L} should replace ψ^{*}_{f} in equation (1), giving

$$\psi^{\mathrm{L}} = \psi^{*}_{\mathrm{f}} = \exp\left(-\mathrm{i}k^{\mathrm{f}}_{\|}\cdot\rho_{\|}\right)\sum_{h,k}\Psi^{\mathrm{f}*}_{h,k}(z)\exp\left[-2\pi\mathrm{i}(hb_1+kb_2)\cdot\rho_{\|}\right]. \tag{7}$$

From equations (5) and (7) it can be seen that

$$k^{\mathrm{L}}_{\|} = -k^{\mathrm{f}}_{\|} \qquad \Psi^{\mathrm{L}}_{h,k}(z) = \Psi^{\mathrm{f}*}_{-h,-k}(z)$$

and accordingly from equation (6)

$${}^{\mathrm{L}}b^{n}_{h,k}(z) = {}^{\mathrm{f}}b^{n*}_{-h,-k}(z)$$

and

$$t^{\mathrm{L}}_{n} = t^{\mathrm{f}*}_{n}.$$

2.3. Initial states

The initial states of the photoemission process are obtained from the multi-slice LEED calculation for energies below the vacuum level using a suitably chosen potential and are constructed as a linear combination of Bloch waves [8]. The boundary conditions for the initial-state wavefunction are modified accordingly since there is no incident wave as in the LEED situation. While the procedure may take more calculation time than direct evaluation of the initial-state Green function [26, 27], the contributions of the individual surface electronic states to the photocurrent are obtained separately, which facilitates the physical interpretation; further the bandstructure incorporating the surface is obtained as a by-product of the photoemission calculation [34].

The wavefunction of an initial state can also be written as an expansion as in equation (5) for the LEED wavefunction, but with superscript i, denoting the initial state of the photoelectron instead of L. The scattering amplitude $\Psi^{\mathrm{i}}_{h',k'}(z)$ for the initial state, in the bulk region, is expressed as a linear combination of Bloch wave amplitudes, as was that of the final state. A pseudopotential is used to calculate the initial states, so different Hamiltonians are used for calculation of the initial and final states, which therefore must be properly aligned in energy when evaluating equation (1). The number of $\Psi^{\mathrm{i}}_{h',k'}(z)$ is dependent on the material being studied [34], and is determined by increasing this number (the number of beams) until a sufficiently accurate bandstructure is obtained.

Specifically, an initial state $\Psi^{m}_{h',k'}$ in the bulk region is formed from the mth Bloch wave with amplitudes ${}^{\mathrm{i}}b^{m-}_{h',k'}$ moving towards the surface from the bulk, and ones with amplitudes ${}^{\mathrm{i}}b^{n+}_{h',k'}$ constituting of those moving away from the surface into the bulk (reflected ones) and of a number of evanescent Bloch waves decreasing into the bulk necessary to match waves at the crystal/vacuum interface. All of these waves have the same energy and reduced $k^{\mathrm{i}}_{\|}$. The initial state $\Psi^{m}_{h',k'}$ is written as

$$\Psi^{m}_{h',k'}(z) = \sum_{n}{}^{\mathrm{i}}b^{n+}_{h',k'}(z)c^{m}_{n} + {}^{\mathrm{i}}b^{m-}_{h',k'}(z)c^{m-}. \tag{8}$$

In matrix notation equation (8) and its derivative can be expressed as

$$\mathbf{U}^m(z) = \mathbf{B}_i^+(z)\mathbf{c}^m + \mathbf{b}_i^{m-}(z)c^{m-} \tag{9}$$

$$\mathbf{U}'^m(z) = \mathbf{B}_i'^+(z)\mathbf{c}^m + \mathbf{b}_i'^{m-}(z)c^{m-}. \tag{10}$$

$\mathbf{B}_i^+$ and $\mathbf{B}_i'^+$ are $N \times N$ matrices containing the Bloch amplitudes and derivatives respectively travelling away from the surface (and $\mathbf{c}^m$ is a column matrix containing their coefficients c_n^m). $\mathbf{b}_i^{m-}$ and $\mathbf{b}_i'^{m-}$ are column matrices containing the Bloch wave amplitudes and derivatives for the mth Bloch wave travelling towards the surface with amplitude c^{m-} (a number).

In the absence of a surface barrier or over-layer, the coefficients c_n^m in the expansion of the scattering amplitude are found by matching the scattering amplitudes and derivatives at $z = 0$ to evanescent waves in the vacuum. The resulting equation for $\mathbf{c}^m$ is

$$\mathbf{c}^m = -\left[\mathbf{B}_i'^+(0) + \mathrm{i}\mathbf{K}\mathbf{B}_i^+(0)\right]^{-1}\left[\mathbf{b}_i'^{m-}(0) + \mathrm{i}\mathbf{K}\mathbf{b}_i^{m-}(0)\right]c^{m-} \tag{11}$$

where $\mathbf{K}$ is a diagonal $N \times N$ matrix containing the normal components of the wave vectors of the N evanescent waves in the vacuum. The value of c^{m-} is evaluated in normalizing the initial state wavefunction (see below).

To include an over-layer or surface barrier, the waves must be matched at both the bulk crystal/over-layer interface and the over-layer/vacuum interface. The equation for the coefficients in this case is given by

$$\mathbf{c}^m = -\left[\mathbf{B}_i'^+(s) - \mathbf{X}\mathbf{Y}^{-1}\mathbf{B}_i^+(s)\right]^{-1}\left[\mathbf{b}_i'^{m-}(s) - \mathbf{X}\mathbf{Y}^{-1}\mathbf{b}_i^{m-}(s)\right]c^{m-} \tag{12}$$

where

$$\mathbf{X} = \Omega_{21}^{\mathrm{S}}(s) - \mathrm{i}\mathbf{K}\Omega_{22}^{\mathrm{S}}(s) \qquad \mathbf{Y} = \Omega_{11}^{\mathrm{S}}(s) - \mathrm{i}\mathbf{K}\Omega_{12}^{\mathrm{S}}(s) \tag{13}$$

and

$$\Omega^{\mathrm{S}}(s) = \begin{pmatrix} \Omega_{11}^{\mathrm{S}}(s) & \Omega_{12}^{\mathrm{S}}(s) \\ \Omega_{21}^{\mathrm{S}}(s) & \Omega_{22}^{\mathrm{S}}(s) \end{pmatrix}.$$

$\Omega^{\mathrm{S}}(s)$ is the Ω-matrix for the surface region with thickness s [34].

2.3.1. Orthogonalization and normalization of the initial states. The final state, determined as described above, is normalized properly in a LEED calculation so that the incident electron has a probability amplitude of one; however the initial states must be orthogonalized and normalized in order to be inserted in equation (1). In the present calculation we can show (cf. [37] and [38]) that as long as the effect of evanescent Bloch waves can be neglected, the wavefunctions given by equation (8) with different indices m can be regarded as forming an orthogonal system of initial states in the space of the half-infinite crystal. The normalization to the delta function of energy leads to the value of c^{m-} given by

$$c^{m-} = \left[(c/\pi)\left(-\partial k_{m-}/\partial E\right)\right]^{1/2} \tag{14}$$

where we have assumed that the Bloch waves are normalized in one unit cell, giving

$$1 = \sum_{h,k} \int_0^c {}^{\mathrm{i}}b_{h,k}^{m-*}(z)\,{}^{\mathrm{i}}b_{h,k}^{m-}(z)\,\mathrm{d}z.$$

c is the unit lattice translation in the z direction. We note that $\partial k_{m-}/\partial E$ in equation (14) is negative since the Bloch waves with amplitudes ${}^{\mathrm{i}}b_{h,k}^{m-}(z)$ are assumed to be moving towards

the surface from the bulk. The quantity $(\partial k_{m-}/\partial E)^{-1}$ is the group velocity of the Bloch electron and can be calculated as [39]

$$\left(\frac{\partial k_{m-}}{\partial E}\right)^{-1} = \frac{\hbar^2}{\mathrm{i}m}\sum_{h,k}\int_0^c {}^{\mathrm{i}}b^{m-}_{h,k}{}^{*}(z)\frac{\partial}{\partial z}{}^{\mathrm{i}}b^{m-}_{h,k}(z)\mathrm{d}z$$

assuming the same normalization of the Bloch wave as above. Hence we may write

$$c^{m-} = \left(-\frac{\pi}{\mathrm{i}c}\frac{\hbar^2}{m}\sum_{h,k}\int_0^c {}^{\mathrm{i}}b^{m-}_{h,k}{}^{*}(z)\frac{\partial}{\partial z}{}^{\mathrm{i}}b^{m-}_{h,k}(z)\mathrm{d}z\right)^{-1/2}.$$

A more detailed analysis of the orthogonalization and normalization is necessary when the contributions of evanescent Bloch waves become significant. This takes place at resonances and near band edges [38].

2.4. Derivation of the photocurrent equation

For simplicity, assuming an orthogonal crystal lattice system, and correspondingly an orthogonal coordinate system (generalization to non-orthogonal systems can easily be done), the photocurrent as expressed in equation (1) is proportional to

$$j(\hat{R}, E) \propto \sum_{\text{occupied } i}\left|\int_x\int_y\int_z \psi_{\mathrm{f}}^{*}\hat{\varepsilon}\cdot\nabla\psi_i\,\mathrm{d}x\,\mathrm{d}y\,\mathrm{d}z\right|^2 \tag{15}$$

where the polarization vector $\hat{\varepsilon}$ is given by

$$\hat{\varepsilon} = \varepsilon_x\hat{\imath} + \varepsilon_y\hat{\jmath} + \varepsilon_z\hat{k} = \sin\alpha\sin\beta\hat{\imath} + \sin\alpha\cos\beta\hat{\jmath} + \cos\alpha\hat{k}.$$

α is the angle between $\hat{\varepsilon}$ and the surface normal and β is defined to be the angle between the parallel component of $\hat{\varepsilon}$ and $\hat{\imath}$.

Substituting into equation (15) the Fourier series expressions for the initial and final states (analogous in form to equations (5) and (7)) leads to,

$$j(\hat{R}, E) \propto \sum_{\text{occupied } i}\left|\int_x\int_y\int_z\sum_{h,k}\Psi^{\mathrm{f}*}_{h,k}(z)\exp\left(-\mathrm{i}k^{\mathrm{f}}_{h,k}\cdot\rho_{\parallel}\right)\hat{\varepsilon}\cdot\nabla\left[\sum_{h',k'}\Psi^{i}_{h',k'}(z)\right.\right.$$
$$\left.\left.\times\exp\left(\mathrm{i}k^{\mathrm{i}}_{h',k'}\cdot\rho_{\parallel}\right)\right]\mathrm{d}x\,\mathrm{d}y\,\mathrm{d}z\right|^2. \tag{16}$$

The two-dimensional real-space vector $\rho_{\parallel}$ can be written out more fully as

$$\rho_{\parallel} = \left(x/|a_1|\right)a_1 + \left(y/|a_2|\right)a_2$$

where $a_{1,2}$ are the direct lattice vectors in the surface plane, and x and y are the real-space distances. Also, in equation (16)

$$k^{\mathrm{f,i}}_{h,k} = \left(k^{\mathrm{f,i}}_{b_1}/|b_1| + 2\pi h\right)b_1 + \left(k^{\mathrm{f,i}}_{b_2}/|b_2| + 2\pi k\right)b_2$$

where $k^{\mathrm{f,i}}_{b_1}$ and $k^{\mathrm{f,i}}_{b_2}$ are the components of the wave vector $k^{\mathrm{f,i}}_{\parallel}$ in the directions b_1 and b_2 respectively. The dot product in equation (16) can then be written as

$$k^{\mathrm{f,i}}_{h,k}\cdot\rho_{\parallel} = \left(k^{\mathrm{f,i}}_{b_1}/|b_1| + 2\pi h\right)x/|a_1| + \left(k^{\mathrm{f,i}}_{b_2}/|b_2| + 2\pi k\right)y/|a_2|.$$

Expanding ∇, equation (16) can be expressed as

$$j(\hat{R}, E) \propto \sum_{\text{occupied i}} \left| \int_x \int_y \int_z \sum_{h,k} \Psi^{\text{f}*}_{h,k}(z) \exp(-\text{i}\boldsymbol{k}^{\text{f}}_{h,k} \cdot \boldsymbol{\rho}_{\parallel}) \sum_{h',k'} \left[\sin\alpha \sin\beta\, 2\pi\text{i} \left(\frac{k^{\text{i}}_{b_1}}{2\pi|b_1|} + h' \right) \right.\right.$$
$$\times \frac{1}{|a_1|} + \sin\alpha \cos\beta\, 2\pi\text{i} \left(\frac{k^{\text{i}}_{b_2}}{2\pi|b_2|} + k' \right) \frac{1}{|a_2|} + \cos\alpha \frac{\partial}{\partial z} \left. \right]$$
$$\left. \times \Psi^{i}_{h',k'}(z) \exp(\text{i}\boldsymbol{k}^{\text{i}}_{h',k'} \cdot \boldsymbol{\rho}_{\parallel}) \text{d}x\, \text{d}y\, \text{d}z \right|^2 .$$

The integral over x and y can be replaced by the delta functions

$$\delta\{[k^{\text{i}}_{b_1}/2\pi|b_1| + h' - (k^{\text{f}}_{b_1}/2\pi|b_1| + h)]/|a_1|\}$$

and

$$\delta\{[k^{\text{i}}_{b_2}/2\pi|b_2| + k' - (k^{\text{f}}_{b_2}/2\pi|b_2| + k)]/|a_2|\}.$$

Therefore, there will be zero photocurrent unless

$$(1/|b_1|)(k^{\text{i}}_{b_1} - k^{\text{f}}_{b_1}) = 2\pi(h - h') \qquad \text{and} \qquad (1/|b_2|)(k^{\text{i}}_{b_2} - k^{\text{f}}_{b_2}) = 2\pi(k - k') \tag{17}$$

that is, unless the parallel component of the wave vector is conserved modulo a surface reciprocal lattice vector. Writing the wave vectors in terms of the reduced zone scheme (superscript R), it can be deduced from equation (17) that $k^{\text{Ri}}_{b_1} = k^{\text{Rf}}_{b_1}$ and similarly for the b_2 component of k, which gives $h' = h + n$ and $k' = k + q$, where n and q are determined from the direction of emission of the photoelectron and the energy. This relationship describes the position of $\boldsymbol{k}^{\text{f}}_{\parallel}$ relative to $\boldsymbol{k}^{\text{i}}_{\parallel}$ in the extended two-dimensional Brillouin zone. Equation (16) can then be written simply as

$$j(\hat{R}, E) \propto \sum_{\text{occupied } i} \left| \sum_{\text{slices } j} \sum_{h,k} \Psi^{\text{f}*}_{h,k}(\Delta z_j) F_{h,k} \Psi^{i}_{h+n,k+q}(\Delta z_j) \right|^2 \tag{18}$$

where the integral over z is evaluated as a sum over the slices Δz_j and

$$F_{h,k} = 2\pi\text{i}\{[(h+n)|b_1| + k^{\text{Ri}}_{b_1}/2\pi] \sin\alpha \sin\beta + [(k+q)|b_2| + k^{\text{Ri}}_{b_2}/2\pi] \sin\alpha \cos\beta$$
$$+ \cos\alpha\, \partial/\partial z\}$$

(for an orthogonal system $1/(|b_1||a_1|) = 1$; similarly for b_2 and a_2).

2.5. Contribution to the photocurrent from the bulk crystal

As mentioned earlier, the crystal is described by a z coordinate with values of $z = 0 \longrightarrow s$ for an over-layer and $z = s \longrightarrow +\infty$ for the bulk crystal. The contribution to the photocurrent from the semi-infinite bulk is given by the integral over $z = s \longrightarrow +\infty$, and is discussed below.

Substituting the Bloch expansions for the initial (equation (8)) and final (as for equation (6) but with superscript f instead of L) states into equation (18), the probability amplitude $\mathcal{A}_{\text{B}}$ of the photocurrent due to the mth initial state in the bulk crystal can be written as (dropping the index m)

$$\mathcal{A}_{\text{B}} = \sum_{\text{bulk slices } j} \left[\sum_{h,k} \left(\sum_{n} {}^{\text{f}}b^{n*}_{h,k}(\Delta z_j) t^{\text{f}*}_{n} \right) \right] \left[F_{h,k} \left(\sum_{n'} {}^{\text{i}}b^{n'+}_{h,k}(\Delta z_j) c_{n'} + {}^{\text{i}}b^{-}_{h,k}(\Delta z_j) c^{-} \right) \right]$$

where normal emission is assumed for simplicity, i.e. n and q in equation (18) are equal to zero. The above equation can be split into two terms

$$\mathcal{A}_1 = \sum_{j=1}^{\infty} \sum_{h,k} \sum_{n} {}^{\mathrm{f}}b_{h,k}^{n\,*}(\Delta z_j) t_n^{\mathrm{f}*} F_{h,k}\, {}^{\mathrm{i}}b_{h,k}^{-}(\Delta z_j) c^{-}$$

and

$$\mathcal{A}_2 = \sum_{j=1}^{\infty} \sum_{h,k} \sum_{n} {}^{\mathrm{f}}b_{h,k}^{n\,*}(\Delta z_j) t_n^{\mathrm{f}*} F_{h,k} \sum_{n'} {}^{\mathrm{i}}b_{h,k}^{n'+}(\Delta z_j) c_{n'} .$$

The contribution from slices lying beyond the first cell can then be expressed in terms of the Bloch functions in the first cell. If there are q slices in the cell and Δz_q denotes the last slice of the cell, then for example, summing the contribution from slices Δz_1, Δz_{q+1}, Δz_{2q+1}, ... occurring in the expression for $\mathcal{A}_1$ leads to (writing k_i, k_f^n for Bloch wave vectors)

$$\sum_{h,k} \sum_{n} \Big[\Big[1 + \exp\big[\mathrm{i}(-k_{\mathrm{f}}^{n\,*} + k_{\mathrm{i}}) \cdot c\big] + \big\{\exp\big[\mathrm{i}(-k_{\mathrm{f}}^{n\,*} + k_{\mathrm{i}}) \cdot c\big]\big\}^2 + \ldots \Big] \Big]$$
$$\times\ {}^{\mathrm{f}}b_{h,k}^{n\,*}(\Delta z_1) t_n^{\mathrm{f}*} F_{h,k}\, {}^{\mathrm{i}}b_{h,k}^{-}(\Delta z_1) c^{-}$$

where c is the lattice period normal to the surface. This is equal to

$$\sum_{h,k} \sum_{n} \frac{1}{1 - \exp[\mathrm{i}(-k_{\mathrm{f}}^{n\,*} + k_{\mathrm{i}}) \cdot c]} \big[{}^{\mathrm{f}}b_{h,k}^{n\,*}(\Delta z_1) t_n^{\mathrm{f}*} F_{h,k}\, {}^{\mathrm{i}}b_{h,k}^{-}(\Delta z_1) c^{-} \big].$$

Repeating this procedure for all of the slices of the bulk cell gives

$$\mathcal{A}_1 = \sum_{h,k} \sum_{n} \frac{1}{1 - \exp[\mathrm{i}(-k_{\mathrm{f}}^{n\,*} + k_{\mathrm{i}}) \cdot c]} \sum_{j=1}^{q} {}^{\mathrm{f}}b_{h,k}^{n\,*}(\Delta z_j) t_n^{\mathrm{f}*} F_{h,k}\, {}^{\mathrm{i}}b_{h,k}^{-}(\Delta z_j) c^{-}.$$

Similarly, the contribution for the second term $\mathcal{A}_2$ becomes

$$\mathcal{A}_2 = \sum_{h,k} \sum_{n} \sum_{n'} \frac{1}{1 - \exp[\mathrm{i}(-k_{\mathrm{f}}^{n\,*} + k_{\mathrm{i}}^{n'}) \cdot c]} \sum_{j=1}^{q} {}^{\mathrm{f}}b_{h,k}^{n\,*}(\Delta z_j) t_n^{\mathrm{f}*} F_{h,k}\, {}^{\mathrm{i}}b_{h,k}^{n'+}(\Delta z_j) c_{n'}.$$

The complete expression for $\mathcal{A}_{\mathrm{B}}$ can then be written as

$$\mathcal{A}_{\mathrm{B}} = \sum_{n} \Bigg(\Delta_n^{-} \sum_{h,k} \sum_{j=1}^{q} {}^{\mathrm{f}}b_{h,k}^{n\,*}(\Delta z_j) t_n^{\mathrm{f}*} F_{h,k}\, {}^{\mathrm{i}}b_{h,k}^{-}(\Delta z_j) c^{-}$$
$$+ \sum_{n'} \Delta_{n,n'}^{+} \sum_{h,k} \sum_{j=1}^{q} {}^{\mathrm{f}}b_{h,k}^{n\,*}(\Delta z_j) t_n^{\mathrm{f}*} F_{h,k}\, {}^{\mathrm{i}}b_{h,k}^{n'+}(\Delta z_j) c_{n'} \Bigg)$$

where

$$\Delta_n^{-} = 1/\big\{1 - \exp[\mathrm{i}(-k_{\mathrm{f}}^{n\,*} + k_{\mathrm{i}}) \cdot c]\big\}$$

and

$$\Delta_{n,n'}^{+} = 1/\big\{1 - \exp[\mathrm{i}(-k_{\mathrm{f}}^{n\,*} + k_{\mathrm{i}}^{n'}) \cdot c]\big\}.$$

The final form of the probability amplitude for the photocurrent (not including surface states or an over-layer/surface barrier) can then be written in terms of LEED functions as

$$\mathcal{A}_B = \sum_n \Bigg(\Delta_n^- \sum_{h,k} \sum_{j=1}^{q} {}^{L}b^n_{-h,-k}(\Delta z_j) t_n^L F_{h,k}\, {}^{i}b^-_{h,k}(\Delta z_j) c^- + \sum_{n'} \Delta^+_{n,n'} \sum_{h,k} \sum_{j=1}^{q} {}^{L}b^n_{-h,-k}(\Delta z_j) t_n^L F_{h,k}\, {}^{i}b^{n'}_{h,k}{}^{+}(\Delta z_j) c_{n'} \Bigg)$$

where

$$\Delta_n^- = 1/\{1 - \exp[\mathrm{i}(\boldsymbol{k}_L^n + \boldsymbol{k}_i) \cdot \boldsymbol{c}]\}$$

and

$$\Delta^+_{n,n'} = 1/\{1 - \exp[\mathrm{i}(\boldsymbol{k}_L^n + \boldsymbol{k}_i^{n'}) \cdot \boldsymbol{c}]\}.$$

The interference between different layers is accounted for by the factors Δ which represent the remnant of the conservation of crystal momentum in the z direction. Only if an infinite number of layers contribute to the photocurrent (i.e. in the unrealistic case of vanishing damping) do the factors Δ reduce to the δ-function-like form. To simulate the effect of inelastic scattering (damping) an imaginary part is added to the energy for both the initial and final states. A value of this parameter can be obtained by various means [40, 41]. Accordingly, the wave vectors are complex in the z direction.

2.6. Contribution to the photocurrent from the surface barrier or over-layer

The contribution $\mathcal{A}_S$ to the probability amplitude of the photocurrent due to the surface barrier or over-layer for a particular initial state is given by

$$\mathcal{A}_S = \sum_{\text{surface slices}}^{m} \sum_{j=1} \sum_{h,k} \Psi^{f*}_{h,k}(\Delta z_j) F_{h,k} \Psi^i_{h,k}(\Delta z_j)$$

where there are m slices in the surface barrier or over-layer. This contribution is added to that, $\mathcal{A}_B$, of the bulk. The values of $\Psi^{f*}_{h,k}$ and $\Psi^i_{h,k}$ in the surface region are obtained using the Ω-matrix formula having determined their values inside the bulk.

2.7. One-dimensional DOS factor

Lastly the sum over 'occupied i' must be considered. This sum implies two factors, one of which was mentioned above, that is, the contribution to the intensity from each initial state (each ${}^{i}b^{m-}_{h',k'}(z)$ in equation (8)) with band index $m-$ must be added together. The second factor is the one-dimensional density of states $\partial k_{m-}/\partial E$ along k_z. We see, however, in equation (14) that this factor is already included in the normalization factor c^{m-} in normalizing the initial-state wavefunctions to the delta function of energy. The total current is then given by

$$j(\hat{R}, E) \propto \sum_{\text{occupied band } (m-)} |\, \mathcal{A}_S^{(m-)} + \mathcal{A}_B^{(m-)} \,|^2 . \tag{19}$$

We note that the contributions from the bands with index $n'+$, corresponding to the Bloch waves moving away from the surface into the bulk, may be obtained by collecting the contributions from the corresponding term in the expression for $\mathcal{A}_2$ above. It can also be shown (cf. [8] and [38]) that the density-of-states factors for these bands are automatically correctly introduced.

2.8. Surface states as initial states

Photoemission is possible from both surface states and surface resonances. Surface resonances occur outside an energy gap and are like surface reflected bulk states with a high amplitude near the surface. Emission from these states are included in the method described above.

Surface states are evanescent waves located at the surface of a crystal, therefore the expression for their scattering amplitudes and derivatives in terms of Bloch waves does not contain any propagating waves, only decreasing components. Neglecting again initially the presence of a surface barrier/over-layer, the surface state wavefunctions are derived from equations (9) and (10), but without the $\mathbf{b}_i^-$ and $\mathbf{b}_i'^-$ terms present. The coefficient vector $\mathbf{c}$ is determined by solving the homogeneous equation

$$\mathbf{Qc} = \mathbf{0} \tag{20}$$

where

$$\mathbf{Q} = \mathbf{B}_i'^+(0) + \mathrm{i}\mathbf{K}\mathbf{B}_i^+(0).$$

A solution will exist if the determinant of $\mathbf{Q}$ is zero, which occurs only at discrete energies. This constitutes a method of obtaining the surface state/resonance bandstructure [34]. Thus, in the present calculation scheme the surface state, as an initial state, must be calculated by a different method to that for bulk states and surface resonances. A convenient way of obtaining the photocurrent due to a surface state with a finite lifetime is as follows.

After equation (1), the photocurrent for a particular initial state ψ_i can be expressed as being proportional to

$$|\langle\psi_f|H^{\mathrm{int}}|\psi_i\rangle|^2\delta(E_f - E_i - \hbar\omega) = \langle\psi_f|H^{\mathrm{int}}|\psi_i\rangle\delta(E_f - E_i - \hbar\omega)\langle\psi_i|H^{\mathrm{int}}|\psi_f\rangle\,.$$

The central part is replaced by [26]

$$|\psi_i\rangle\delta(E - E_i)\langle\psi_i| = -(1/\pi)\Im m\, G_i(E)$$

where $E = E_f - \hbar\omega$ and $G_i(E)$ is the ith spectral component of the Green function

$$G_i(E) = |\psi_i\rangle\langle\psi_i|/\big(E - E_i + \mathrm{i}\varepsilon_i\big) \qquad \big(\varepsilon_i \longrightarrow +0\big)$$

giving

$$j(\widehat{R}, E) \propto -(1/\pi)\langle\psi_f|H^{\mathrm{int}}|\Im m\, G_i(E)|H^{\mathrm{int}}|\psi_f\rangle. \tag{21}$$

To introduce a finite lifetime we impose on ε_i a finite value. Then a surface state $|\psi_i\rangle$ appears at energy E_i with lifetime parameter ε_i. It is desired to find an approximate expression for $G_i(E)$ for values of E near E_i.

In place of equation (20) a more general equation can be written:

$$\mathbf{Q}(E)\mathbf{c}(E) = \mu(E)\mathbf{c}(E) \tag{22}$$

where $\mu(E)$ and $\mathbf{c}(E)$ are the eigenvalue and eigenvector of $\mathbf{Q}(E)$ respectively. Equation (22) indicates that one of the eigenvalues, $\mu_i(E)$, becomes equal to zero at $E = E_i$. (This is equivalent to $\det\mathbf{Q} = 0$, because $\det\mathbf{Q}$ is equal to the product of the eigenvalues of $\mathbf{Q}$). Expanding $\mu_i(E)$ in a Taylor series around E_i

$$\mu_i(E) = (\mathrm{d}\mu_i/\mathrm{d}E)_{E=E_i}(E - E_i) + \ldots.$$

Then writing

$$(E - E_i) = (\mathrm{d}\mu_i/\mathrm{d}E)^{-1}_{E=E_i}\mu_i(E)$$

and substituting it into the expression for $G_i(E)$

$$G_i(E) = |\psi_i\rangle\langle\psi_i|/\left\{\left[(\mathrm{d}\mu_i/\mathrm{d}E)_{E=E_i}\right]^{-1}\mu_i(E) + \mathrm{i}\varepsilon_i\right\}.$$

The eigenvector of $\mathbf{Q}(E)$ which belongs to the eigenvalue $\mu_i(E)$ is designated $\mathbf{c}_i(E)$. The value of $\mathbf{c}$ which is sought as a solution of equation (20) is simply the value of $\mathbf{c}_i(E)$ at $E = E_i$. Hence

$$|\psi_i\rangle = |c\rangle = |c_i(E_i)\rangle.$$

The symbol $|c\rangle$ means a linear combination of Bloch functions with coefficients c_n. Hence

$$G_i(E) = |c_i(E_i)\rangle\langle c_i(E_i)|/\left\{\left[(\mathrm{d}\mu_i/\mathrm{d}E)_{E=E_i}\right]^{-1}\mu_i(E) + \mathrm{i}\varepsilon_i\right\}.$$

$|c_i(E_i)\rangle$ should be normalized in such a way that the integral of the absolute square of the wavefunction ψ_i over the two-dimensional unit cell and the range of z in which ψ_i is finite (including the vacuum region) becomes unity. In the present notation the integral is evaluated as

$$(\psi_i, \psi_i) = \sum_{\text{slices } j}\sum_{h,k} \Psi^{i\,*}_{h,k}(\Delta z_j)\Psi^{i}_{h,k}(\Delta z_j)$$

where $\Psi^i_{h,k}(z) = \sum_n {}^{\mathrm{i}}b^{n+}_{h,k}(z)c_n$ in the bulk crystal. Their values in the surface and vacuum regions are derived by the Ω-matrix method (as in section 2.6).

Since the values of $\mathrm{d}\mu_i/\mathrm{d}E$ and c_i may not vary appreciably in the small energy range of a surface state peak breadth, their actual values may be replaced by their approximate values evaluated at an energy $E = E_i'$ near E_i. Thus, an exact value of E_i need not be found. Then $G_i(E)$ can be written as

$$G_i(E) = |c_i(E_i')\rangle\langle c_i(E_i')|/\left\{\left[(\mathrm{d}\mu_i/\mathrm{d}E)_{E=E_i'}\right]^{-1}\mu_i(E) + \mathrm{i}\varepsilon_i\right\}. \tag{23}$$

This equation can be evaluated by firstly approximately locating the surface state by finding either the zeros of $\mathbf{Q}$ or the minima of μ that are most conveniently located by considering instead the Hermitian matrix $\mathbf{Q}^\dagger\mathbf{Q}$ and finding the minima of the corresponding eigenvalues $|\mu|^2$. Once located at energy E_i', μ is obtained for a small region of energy around the surface state from which the denominator of equation (23) can be evaluated. The eigenvectors of equation (22) give $|c_i(E_i')\rangle$. $G_i(E)$ is then evaluated and substituted into equation (21) to obtain the photocurrent due to the surface state.

3. Application to Mg(0001)

As a numerical example, the method presented above is applied to the calculation of normal-emission photoemission intensities from Mg(0001) in the photon energy range $\hbar\omega$ = 26–48 eV where the results obtained are compared to the experimental data of Bartynski *et al* [42] (figure 2). Figure 1(a) and (b) shows respectively the experimental and theoretical results. The main features in the experimental results are a surface-state peak which occurs in all the spectra at approximately −1.6 eV, and a bulk transition seen initially at approximately

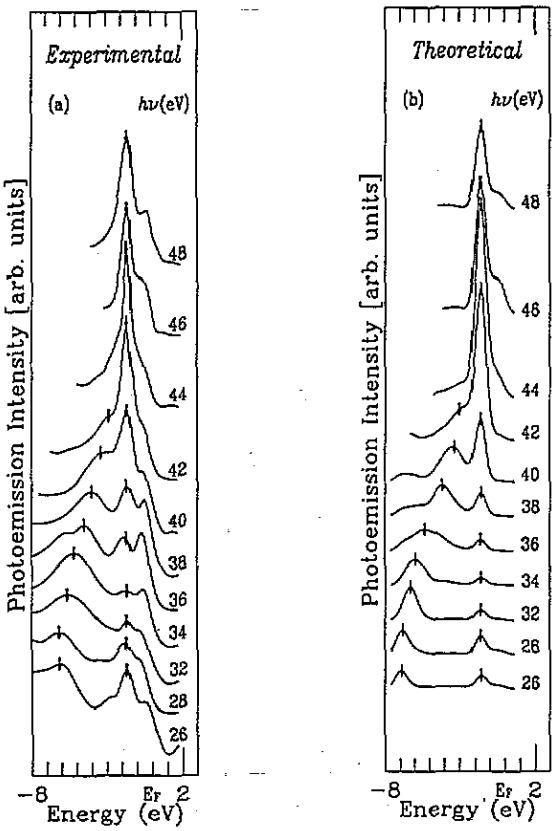

Figure 1. (a) Experimental normal-emission photoemission spectra from the Mg(0001) surface for various photon energies, reproduced from [42]; (b) calculated photoemission intensities obtained using the present method.

−6.2 eV for $\hbar\omega = 26$ eV. The latter peak disperses towards the Fermi level with increasing photon energy. At $\hbar\omega \simeq 44$ eV this peak coincides with the surface-state peak.

The theoretical results show reasonable agreement with the experimental results, where a surface state occurs at approximately −1.6 eV. The corresponding bulk transition is seen at about −6.9 eV for $\hbar\omega = 26$ eV and disperses towards the Fermi level with increasing photon energy as in the experimental results. The theoretical spectra were calculated using a three-dimensional surface potential barrier (both at initial state and final state energies) in which the potential smoothly goes to zero in the vacuum region. It was obtained using a supercell consisting of eight Mg layers (20.8 Å) and a vacuum region corresponding to the same distance [32].

It can be seen when comparing the theoretical spectra with the experimental data that the bulk transition is shifted non-uniformly. The origin of this discrepancy could be due to either deficiencies in the local-density approximation used in the band calculations or to inaccuracies inherent in comparing an excitation spectrum with a ground-state calculation (the self-energy effect).

The surface-state intensities of both the experimental and theoretical results exhibit a sensitive variation with photon energy. This is illustrated in figure 2 in which the experimental points have been reproduced from [42] (figure 3) and are shown as filled

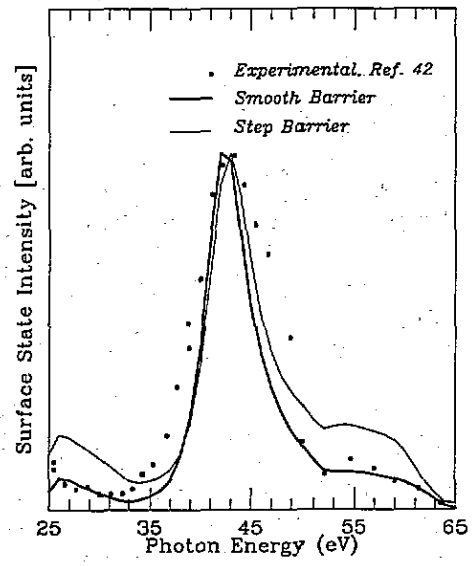

Figure 2. Comparison of the surface-state intensity as a function of photon energy. The filled circles are the experimental results taken from [42]; the fine curve is the calculated intensity obtained using a step barrier and the bold curve is the calculated intensity obtained using a smooth surface barrier.

circles. The theoretical points, obtained using equation (21), are shown as the curves. The fine curve is the result obtained using a step barrier placed half way between Mg atoms and for the bold curve the same smooth surface barrier as in figure 1(b) is used. It can be seen that the smooth barrier yields results that agree better with experiment, illustrating the importance of including a realistic surface potential barrier when surface effects in photoemission are being investigated. The results briefly presented above will be discussed in more detail in a subsequent publication [32].

4. Conclusion

It is shown that a one-step photoemission calculation scheme can be presented in a formulation based on the multi-slice method of determining LEED intensities. It is applicable for electrons in the valence band region and takes account of final-state and surface effects and electron and hole lifetimes. Emission from bulk and surface states are calculated separately in the present procedure. This method has been successfully applied to magnesium and gallium arsenide, the results of which will appear in subsequent papers [32,33].

Acknowledgments

C Stampfl would like to thank both the Education Department of Australia for a Commonwealth Postgraduate Award and the Deutscher Akademisher Austauschdienst (DAAD) for a research grant, and Professor M Scheffler for use of the facilities at the Fritz-Haber-Institut where part of the present work was carried out. Professor R Leckey is also thanked for helpful discussions.

References

[1] Berglund C N and Spicer W E 1964 *Phys. Rev.* **136** A1030
[2] Smith N V 1980 *Phys. Rev.* B **21** 4331
[3] Jepsen D W, Himpsel F J and Eastman D E 1982 *Phys. Rev.* B **26** 4039
[4] Adawi I 1964 *Phys. Rev.* **134** A788
[5] Mahan G D 1970 *Phys. Rev. Lett.* **24** 1068; 1970 *Phys. Rev. B* **2** 4334
[6] Schaich W L and Ashcroft N W 1971 *Phys. Rev.* B **3** 2452
[7] Caroli C, Lederer-Rozenblatt D, Roulet B and Saint-James D 1973 *Phys. Rev.* B **8** 4552
[8] Feibelman P J and Eastman D E 1974 *Phys. Rev.* B **10** 4932
[9] Feibelman P J 1974 *Surf. Sci.* **46** 558
[10] Liebsch A 1974 *Phys. Rev. Lett.* **32** 1203
[11] Ackermann B and Feder R 1985 *Solid State Commun.* **54** 1077
Ackermann B and Feder R 1985 *J. Phys. C: Solid State Phys.* **18** 1093
[12] Almbladh C O 1985 *Phys. Scr.* **32** 341
[13] Bardyszewski W and Hedin L 1985 *Phys. Scr.* **32** 439
[14] Durham P J 1981 *J. Phys. F: Met. Phys.* **11** 2475
[15] Borstel G and Thörner G 1988 *Surf. Sci. Rep.* **8** 1
[16] Malmström G and Rundgren J 1980 *Comput. Phys. Commun.* **19** 263
[17] Grass M, Braun J and Borstel G 1993 *J. Phys.: Condens. Matter* **5** 599
[18] Blyth R I R, Barrett S D, Dhesi S S, Cosso R, Heritage N, Begley A M and Jordan R G 1991 *Phys. Rev.* B **44** 5423
[19] König U, Blügel S, Redinger J and Weinberger P 1991 *Phys. Rev.* B **43** 1954
[20] Thörner G and Borstel G 1984 *Phys. Status Solidi* b **126** 617
Braun J, Thörner G and Borstel G 1985 *Phys. Status Solidi* b **130** 643
Braun J, Thörner G and Borstel G 1987 *Phys. Status Solidi* b **144** 609
[21] Ginatempo B, Durham P J and Gyorffy B I 1989 *J. Phys.: Condens. Matter* **1** 6483
[22] Halilov S V, Tamura E, Meinert D, Gollisch H and Feder R 1993 *J. Phys.: Condens. Matter* **5** 3859
[23] Larsson C G and Pendry J B 1981 *J. Phys. C: Solid State Phys.* **14** 3089
[24] Braun J, Borstel G and Nolting W 1992 *Phys. Rev.* B **46** 3510
[25] Grass M, Braun J and Borstel G 1993 to be published
[26] Pendry J B 1976 *Surf. Sci.* **57** 679
[27] Hopkinson J F L, Pendry J B and Titterington D J 1980 *Comput. Phys. Commun.* **19** 69; 1983 *Comput. Phys. Commun.* **29** 417
[28] Pendry J B 1981 *J. Phys. C: Solid State Phys.* **14** 1381
[29] Tournarie M 1962 *J. Phys. Soc. Japan* **17** Suppl. B-II 98
[30] Cowley J M and Moodie A F 1957 *Acta Crystallogr.* **10** 609
[31] Martinez G, Schlüter M and Cohen M L 1975 *Phys. Rev.* B **11** 660
[32] Stampfl C, Kambe K and Riley J D to be published
[33] Stampfl C, Kambe K and Riley J D to be published
[34] Stampfl C, Kambe K, Riley J D and Lynch D F 1992 *J. Phys.: Condens. Matter* **4** 8461
[35] Courths R and Hüfner S 1984 *Phys. Rep.* **112** 54
[36] Lynch D L and Moodie A 1972 *Surf. Sci.* **32** 422
[37] Wachutka G 1987 *Phys. Rev.* B **36** 4725
[38] Kambe K to be published
[39] Achcroft N and Mermin N 1976 *Solid State Physics* (New York: Holt, Rinehart and Winston) appendix E
[40] Smith A E 1984 *Phys. Status Solidi* b **123** 619
[41] Pendry J B 1974 *Low Energy Electron Diffraction: The Theory and its Application to Determination of Surface Structure* (London: Academic)
[42] Bartynski R A, Gaylord R H, Gustafsson T and Plummer E W 1986 *Phys. Rev.* B **33** 3644